# Predictive direct torque control with reduced ripples and fuzzy logic speed controller for induction motor drive

Abdelkarim Ammar, Billel Talbi, Tarek Ameid, Younes Azzoug, Abdelaziz Kerrache, Amor Bourek, Abdelhamid Benakcha

# Predictive Direct Torque Control with Reduced Ripples and Fuzzy Logic Speed Controller for Induction Motor Drive

Abdelkarim AMMAR*[1], Billel TALBI[2], Tarek AMEID[1], Younes AZZOUG[1], Abdelaziz KERRACHE[3], Amor BOUREK[1] and Abdelhamid BENAKCHA[1]
[1]Electrical engineering laboratory of Biskra LGEB, University of Biskra, Biskra, Algeria
[2]Laboratory of power electronics and industrial control, University of Sétif 1, Sétif, Algeria.
[3]Electrical engineering Laboratory of ENP Algiers (LRE), National Polytechnic School (ENP), Algiers, Alegria
ammar.abdelkarim@yahoo.fr; bilel_ei@live.fr; tarek-gnr@hotmail.fr ; azzougyounes@yahoo.fr; azizkarrach@gmail.com

***Abstract*** **The direct torque control (DTC) suffers from high torque and flux ripples due to the use of hysteresis comparators. In this paper, an alternative method is presented for induction motor drive known by the model Predictive Torque Control (PTC). This technique includes the inverter model in control design and does not use any modulation block. The optimal selection of inverter switching states minimizes the error between references and the predicted values of control variables by the optimization of a cost function. Consequently, it reduces ripples and solve DTC drawbacks. Furthermore, this paper proposes an improvement in the external speed loop for PTC scheme. A fuzzy logic controller replaces the traditional PI controller to ensure more accurate speed tracking and increase the robustness against disturbance and uncertainties. The effectiveness of the presented algorithms is investigated by an experimental implementation with the aid of real-time interface (RTI) based on dSpace 1104.**

**Keywords— Induction Motor (IM), Direct Torque Control (DTC), Predictive Torque Control (PTC), Fuzzy Logic Controller, dSpace 1104.**

## I. INTRODUCTION

The Direct Torque Control (DTC) replaces the field oriented control (FOC) in high performance AC machines drive field [1], [2]. DTC offers a simpler scheme, faster response and less dependence to machine parameters. However, due to the use of hysteresis comparators for flux and torque control; a look-up switching table for voltage vector selection, the strategy shows high ripples and harmonics. They can lead to an acoustical noise and decrease the performance of the controlled machine especially at low speed regions.

In order to overcome the aforementioned problems and improve the performances of DTC, various proposed solution have been presented in the last few decades, such as multilevel converters, artificial intelligence techniques [3] and fixed switching frequency modulation techniques like the space vector modulation (SVM)[4]. SVM preserves a constant switching frequency which can reduce torque/flux ripples and switching losses. However, the application of SVM can increase control algorithm complexity which lead to an extensive software/hardware computational requirement.

Recently, another method has been introduced and attracted a wide attention in the area of power converters and motor drives which is known by the Model Predictive Control (MPC) [5], [6]. Nowadays, MPC has become a very popular research topic. It can be classified into two main categories, named by continuous and finite-state model predictive control (FS-MPC) [7]. The continuous MPC can demonstrate good performance but it has high order of complexity and needs a modulator in control design (i.e. pulse width modulator (PWM) or space vector modulator (SVM)) [8]. Contrariwise, FS-MPC eliminates the use of modulation block, it incorporates the converters model in the control design and respects its discrete nature [5]. The switching states are considered in order to minimize a predefined cost function which consists of the errors between references and predicted measured control variables.

The main applied finite-state model predictive control strategies for IM drive, are the predictive current control (PCC) and the predictive torque control (PTC) which have been proposed for the first time in 2007 [5], [6]. PCC is expressed in the rotor field oriented reference where the coordinates transformation is a necessary process, whilst, PTC is featured by stationary reference frame. Hence, it is much simpler and keeps similar structure of traditional DTC, where the switching table is replaced by the online optimization procedure[9]. In finite state PTC (FS-PTC), torque and stator flux are predicted for the finite number of possible switching states of a power converter. The optimal choice of switching states which is obtained by actuating the cost function can reduce torque and flux ripples, therefore it can overcome the main DTC drawback. Then, the selected state is directly applied to the converter in the next sampling instant [10].

FS-PTC is also a closed-loop adjustable speed drive, where, the measured rotor speed is required as a feedback and compared to reference value for PI controller design. Another objective of this paper is to improve the speed control of PTC by a fuzzy logic controller (FLC). FLC can offer good response and accurate tracking without need the knowledge of the exact system model [11]. Therefore, it will be used in this work instead of PI controller in the external loop for speed regulation and torque reference generation.

In this paper, a predictive torque control is presented for the goal of torque and flux ripple reduction. In addition, a fuzzy logic controller is associated in the external loop for speed regulation. The presented methods will be investigated through an experimental verification using Matlab/Simulink software with real-time interface (RTI) based on dSpace 1104.

## II. Induction Machine and Voltage Inverter Models

### A. IM Model

The dynamic equation's model of the induction machine can be expressed by the following complex form in the stator reference frame, (1), (2) and (3) present voltage, flux and electromagnetic equations respectively:

$$\begin{cases} \bar{v}_s = R_s \bar{i}_s + \dfrac{d\bar{\psi}_s}{dt} \\ 0 = R_r \bar{i}_r + \dfrac{d\bar{\psi}_r}{dt} - j\omega_r \bar{\psi}_r \end{cases} \quad (1)$$

$$\begin{cases} \bar{\psi}_s = L_s \bar{i}_s + M_{sr} \bar{i}_r \\ \bar{\psi}_r = M_{sr} \bar{i}_s + L_r \bar{i}_r \end{cases} \quad (2)$$

$$T_e = p \cdot \mathrm{Im}\left\{\bar{\psi}_s \cdot \bar{i}_s\right\} \quad (3)$$

Where:

$\bar{v}_s$ is the stator voltage vector;

$\bar{\psi}_s$ and $\bar{\psi}_r$ are the stator flux and rotor flux.

$\bar{i}_s$ and $\bar{i}_r$ are the stator and rotor currents.

$R_s$ and $R_r$ are the stator and rotor resistances.

$Ls$, $Lr$ and $Msr$ are stator, rotor and mutual inductance.

$\omega_r$ is the electrical velocity and $p$ is the number of pole pairs.

### B. Two-Level Voltage Source Inverter Model

In this work, a two-level voltage source inverter (VSI) fed the controlled IM. The voltage vector is generated by the following expression:

$$V_s = \sqrt{\frac{2}{3}} V_{dc} \left[ S_a + S_b e^{j\frac{2\pi}{3}} + S_c e^{j\frac{4\pi}{3}} \right] \quad (4)$$

$V_{dc}$: is the DC link voltage

The inverter's control bases on the logic values $S_i$, where:

$S_i$=1, $T_i$ is ON and $\overline{T_i}$ is OFF.

$S_i$=0, $T_i$ is OFF and $\overline{T_i}$ is ON.

with: $i$= *a, b, c.*

There are eight possible positions from the combinations of switching states. Six are active vectors (*V1, V2 ... V6*) and two are zero vectors (*V0, V7*). These eight switching states are shown as space vectors in Fig.1.

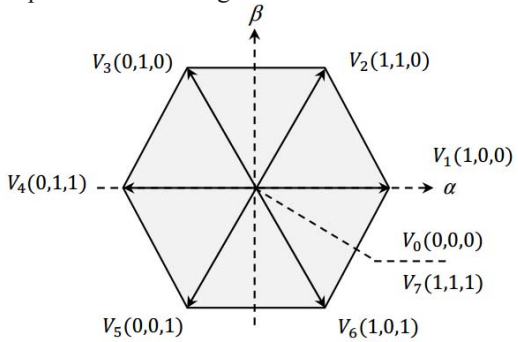


Fig.1 Two-level VSI voltage vectors in the complex plane.

## III. Basic Direct Torque Control

Direct torque control achieves a decoupled control of the stator flux and the electromagnetic torque in the stationary frame. The selection of the switching states is made by restricting the flux and torque magnitudes within two hysteresis bands. The outputs of hysteresis comparators with the aid of lookup switching table determine an appropriate voltage vector for each commutation period [12].

## IV. Finite-State Predictive Torque Control (FS-PTC)

FS-PTC algorithm includes three main steps, the flux and torque estimation is first step. The second step is the prediction of the next-instant of current $\bar{i}_s(k+1)$, flux $\hat{\bar{\psi}}_s(k+1)$ and torque $\hat{T}_e(k+1)$. The cost function optimization design is done finally[13].

### A. Stator Current, Flux and Electromagnetic Prediction

From the IM model, the stator current and the stator flux can be described as follows:

$$\frac{d\hat{\bar{\psi}}_s}{dt} = \bar{v}_s - R_s \bar{i}_s \quad (5)$$

$$\bar{i}_s = -\frac{1}{R_\sigma}\left( L_\sigma \cdot \frac{d\bar{i}_s}{dt} - k_r \cdot \left( \frac{1}{T_r} - j\omega \right) \bar{\psi}_r \right) - \bar{v}_s \quad (6)$$

Where:

$k_r = M_{sr}/L_r$, $R_\sigma = R_s + k_r^2 \cdot R_r$, $L_\sigma = \sigma L_s$

To predict the required signals (currents, flux and torque) into the next step, the Euler forward discretization equation is used:

$$\frac{dx}{dt} \approx \frac{x(k+1) - x(k)}{T_z} \quad (7)$$

After discretization with the sampling time $T_z$, the stator flux prediction can be obtained as:

$$\hat{\bar{\psi}}_s(k+1) = \hat{\bar{\psi}}_s(k) + T_z \bar{v}_s(k) - R_s \cdot T_z \bar{i}_s(k) \quad (8)$$

The stator flux prediction can be obtained as:

$$\bar{i}_s(k+1) = \left(1 - \frac{T_z}{T_\sigma}\right) \cdot \bar{i}_s(k) + \frac{T_z}{T_\sigma} \cdot \frac{1}{R_\sigma}\left( k_r \cdot \left( \frac{1}{T_r} - j\omega(k) \right) \bar{\psi}_r(k) + \bar{v}_s(k) \right) \quad (9)$$

with

$T_\sigma = \sigma L_s / R_\sigma$

By the predictions of the stator flux and current, the electromagnetic torque can be predicted as following:

$$\hat{T}_e(k+1) = p \cdot \mathrm{Im}\left\{ \hat{\bar{\psi}}_s(k+1) \cdot \bar{i}_s(k+1) \right\} \quad (10)$$

### B. Voltage vector selection

The cost function in the MPC strategy compares the predicted and reference values[7]. The classical cost function for the PTC method is:

$$g = \left| T_e^* - \hat{T}_e(k+1) \right| + \lambda \left| \bar{\psi}_s^* - \hat{\bar{\psi}}_s(k+1) \right| \quad (11)$$

where $T_e^*$ is the reference torque and $\hat{T}_e(k+1)$ is the predicted torque for a given switching state, $\bar{\psi}_s^*$ is the reference stator flux and $\hat{\bar{\psi}}_s(k+1)$ is the predicted stator flux, and $\lambda$ is the weighting factor which defines a trade-off between the torque and flux tracking [10].

Various approaches have been presented for solving weighting factor choosing problem. In this work, a modified cost function is considered as presented in [14]. This method modifies the expression (11) into the following (12):

$$g = \frac{1}{T_{en}^2}\left|T_e^* - \hat{T}_e(k+1)\right| + \frac{\lambda}{\psi_{sn}^2}\left|\bar{\psi}_s^* - \hat{\bar{\psi}}_s(k+1)\right| \quad (12)$$

$T_{en}$ and $\psi_{sn}$ are the rated values for the torque and flux, respectively.

### C. Cost Function Extensions in FS-PTC Algorithm

In FS-PTC, the cost function can be extended by adding other control objectives and system constraints. For example, current limitation term $I_m$ is added in order to protect over current through the stator. This term is designed according to the maximum supportable current by the machine [10], [15] as following:

$$I_m = \begin{cases} \infty, & if \ \left|\bar{i}_s(k+1)\right| > i_{\max} \\ 0, & if \ \left|\bar{i}_s(k+1)\right| \le i_{\max} \end{cases} \quad (13)$$

$i_{max}$ is the maximum current rating of the IM. Thus, the complete cost function $g$ for the controller is:

$$g = \frac{1}{T_{en}^2}\left|T_e^* - \hat{T}_e(k+1)\right| + \frac{\lambda}{\psi_{sn}^2}\left|\bar{\psi}_s^* - \hat{\bar{\psi}}_s(k+1)\right| + I_m \quad (14)$$

### D. Time-Delay Compensation

In simulation, the speed and stator current measurements are taken at the discrete instant $k$, and at the same time the optimum voltage vector $\bar{v}_s(k)$ is applied to the machine. However, in experimental, the processor needs time to execute the algorithm[13] . Hence, to implement a delay time compensation, the predicted stator flux, current and torque at instant $k + 2$ are obtained by:

$$\hat{\bar{\psi}}_s(k+2) = \hat{\bar{\psi}}_s(k+1) + T_z\bar{v}_s(k+1) - R_s \cdot T_z\bar{i}_s(k+1) \quad (15)$$

$$\bar{i}_s(k+2) = \left(1 - \frac{T_z}{T_\sigma}\right)\cdot \bar{i}_s(k+1) + \frac{T_z}{T_\sigma}\cdot \frac{1}{R_\sigma}\left(k_r \cdot \left(\frac{1}{T_r} - j\,\omega(k)\right)\bar{\psi}_r(k+1) + \bar{v}_s(k+1)\right) \quad (16)$$

$$\hat{T}_e(k+2) = p \cdot \mathrm{Im}\left\{\hat{\bar{\psi}}_s(k+2)\cdot \bar{i}_s(k+2)\right\} \quad (17)$$

By considering the calculation delay in real time implementation, the cost function become:

$$g = \frac{1}{T_{en}^2}\left|T_e^* - \hat{T}_e(k+2)\right| + \frac{\lambda}{\psi_{sn}^2}\left|\bar{\psi}_s^* - \hat{\bar{\psi}}_s(k+2)\right| + I_m \quad (18)$$

## V. FUZZY LOGIC SPEED CONTROLLER DESIGN

In this section, a fuzzy logic controller is designed to replace the PI controller and generate the reference's torque. FLC is featured that it does not require an exact modeling or identification [11]. The tracking error and its time derivative are considered as the input variables. The rotor speed error is defined by:

$$e_{\omega_r} = \omega_r^* - \omega_r \quad (19)$$

There are seven variables for the input variables, defined in the fuzzy sets: PB (positive big), PM (positive medium), PS (positive small), Z (zero), NS (negative small), NM (negative medium), and NB (negative big). Extra variables are added in the fuzzy sets for the output (PMB, PMS, NMB, NMS) to improve the dynamic performance and obtain more refined output. Figs.2-3 present the membership functions of the inputs and the outputs.

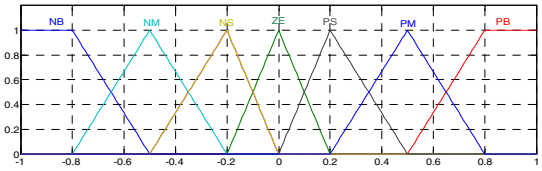


Fig.2. Input membership function.

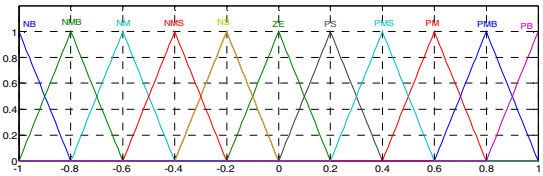


Fig.3. Output membership function.

Table.I shows the inference rule implemented in this paper, which is the important part of the FLC.

TABLE. I Fuzzy Rules Base

| e / ce | NB | NM | NS | ZE | PS | PM | PB |
|---|---|---|---|---|---|---|---|
| NB | NB | NB | NBM | NM | NMS | NS | ZE |
| NM | NB | NBM | NM | NMS | NS | ZE | PS |
| NS | NBM | NM | NMS | NS | ZE | PS | PMS |
| ZE | NM | NMS | NS | ZE | PS | PMS | PM |
| PS | NMS | NS | ZE | PS | PMS | PM | PBM |
| PM | NS | ZE | PS | PMS | PM | PBM | PB |
| PB | ZE | PS | PMS | PM | PBM | PB | PB |

Fig.4 show the global diagram of predictive direct torque control associated to fuzzy logic speed controller.

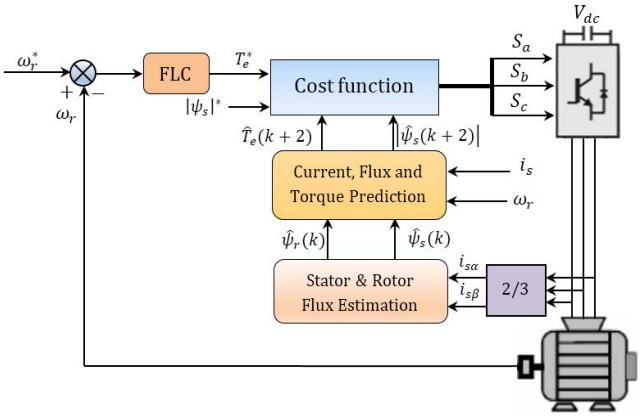


Fig.4 Diagram of predictive torque control with fuzzy logic speed controller for IM drive.

## VI. Experimental Results

### A. Test bench presentation

The real-time implementation was done in the laboratory equipped by dSpace 1104 interface.

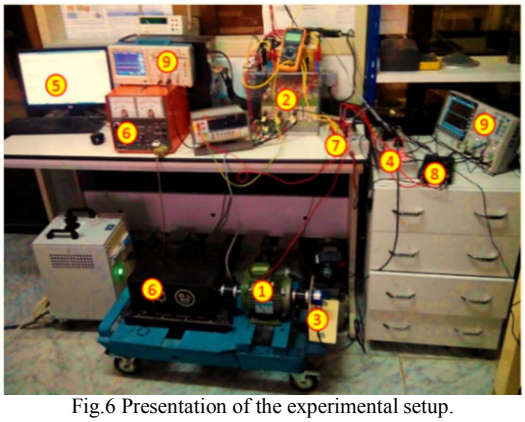


Fig.6 Presentation of the experimental setup.

The experimental test bench of IM drive is composed as presented in (Fig.6) of: 1: A squirrel-cage IM *1.1 kW*. 2: power electronics Semikron converter composed of a rectifier and an IGBT based voltage source inverter. 3: position and speed sensor (type: incremental encoder). 4: dSpace dS 1104 with 5: Matlab/Simulink/Controldesk software plugged in personal computer. 6: magnetic powder brake with load control unit. 7: Hall type current sensors.8: DC-bus voltage sensors. 9: numerical oscilloscope.

The results have been extracted using GW-INSTEK numerical oscilloscope which is linked to the real-time interface. The performance analysis of PTC strategy is done through the comparison to a conventional switching table DTC strategy (ST-DTC). Besides, the FLC controller in speed loop is compared to traditional PI.

### B. ST-DTC and PTC Comparative Analysis

This section presents a comparative analysis of the presented predictive torque control with the conventional DTC. To verify the effectiveness of both control schemes, different operation conditions have been performed, such as: steady state, speed sense reversal and load application.

The figures are specified by (a) for switching table based DTC (ST-DTC) and (b) for predictive torque control (PTC).

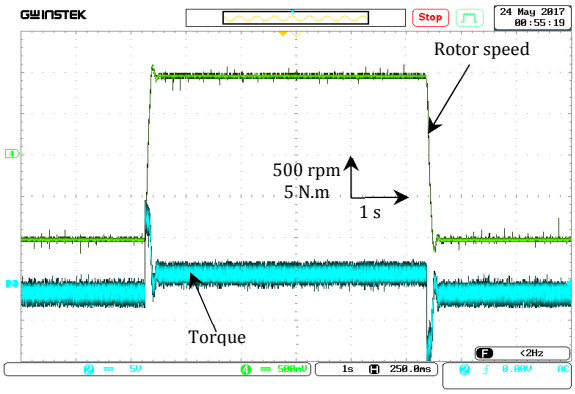


(a) ST-DTC

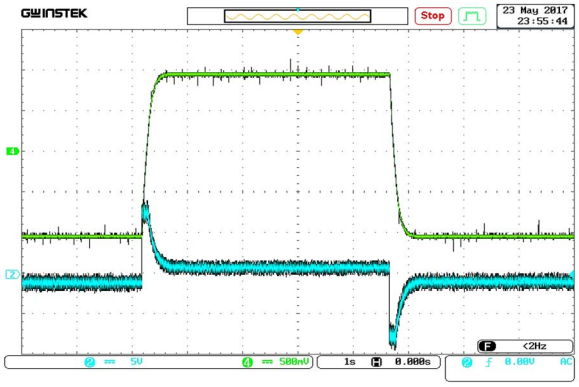


(b) PTC

Fig.7 Rotor speed and torque responses as a reversal maneuver.

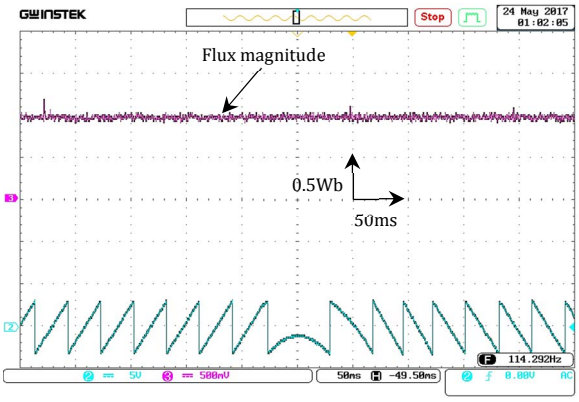


(a) ST-DTC

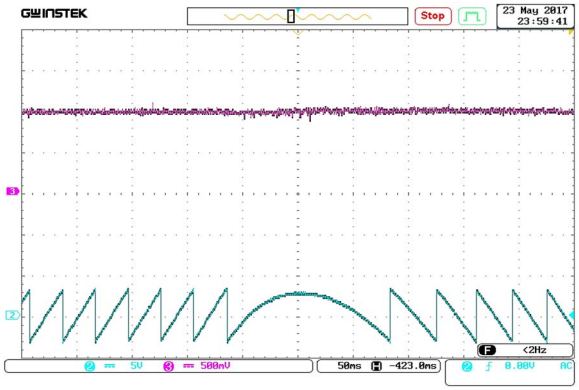


(b) PTC

Fig.8 Stator flux magnitude and position during the reversal maneuver.

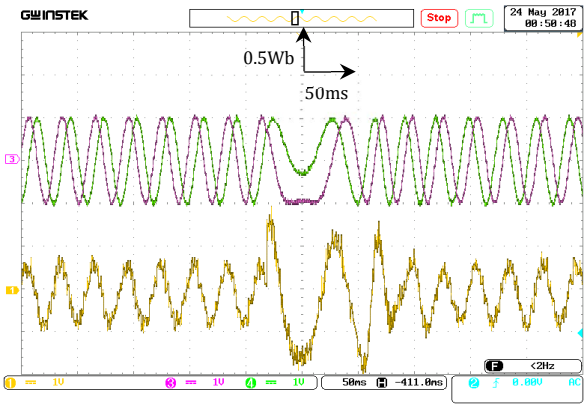


(a) ST-DTC

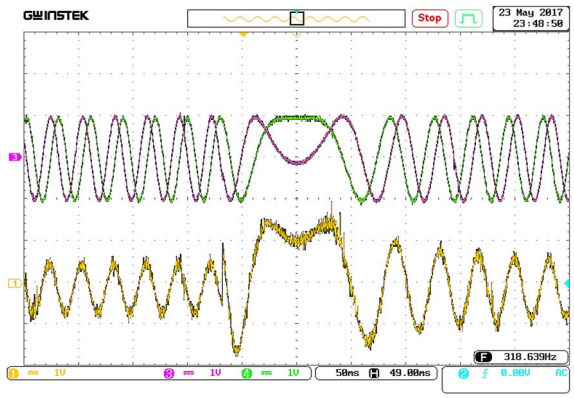

(b) PTC

Fig.9. Stator flux components and stator current during the sense reversal.

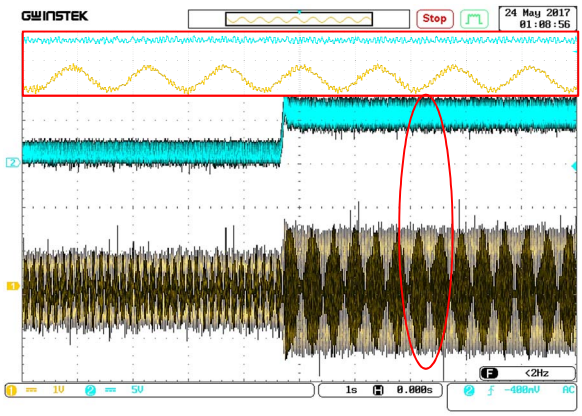

(a) ST-DTC

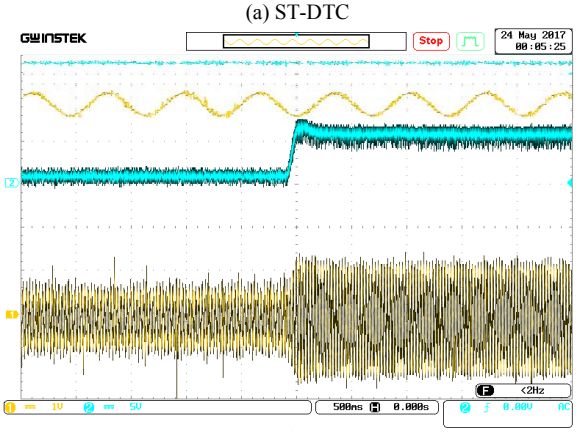

(b) PTC

Fig.10 Electromagnetic torque and stator current during load application.

The first presented test in Fig.7 illustrates speed and torque responses during steady state and rotation sense reversing of (*1000 rpm* to *– 1000 rpm*). Both control strategies show a good speed and torque dynamic. It can be seen clearly in Fig.7(b) that PTC provides a considerable reduction in torque ripples compared to ST-DTC in Fig.7(b). Next, in Fig.8 the stator flux magnitude and its position are depicted. By comparison Fig.8(a) and Fig.8(b) we can see that PTC reduce the flux ripples also. The flux position has been added to indicate the sense reversal. From Figs.7-8 we can see that PTC has reduced apparently the torque and flux ripples which is the main drawback of ST-DTC. The exhibited results in Fig.9 present the stator flux components in the stationary frame and the stator phase current. In Fig.9(a), DTC presents a distorted form of flux and current waveforms which indicate to the high level of harmonics, contrariwise, PTC in Fig.9(b) presents a smoother flux and better current sinusoids waveforms. Then in Fig.10, a load disturbance of 5 N.m has been introduced, the figure shows the electromagnetic torque and stator phase current during load application. Both of control technique responds to load disturbance quickly, we can observe the better current waveform and the big reduction in torque ripples for PTC in this condition also.

### *C. PI and FLC Speed Controllers Performance Analysis*

This section exhibits a comparison of PI and FLC in the external speed loop of PTC strategy. The figures are specified by (a) for PI and (b) for FLC.

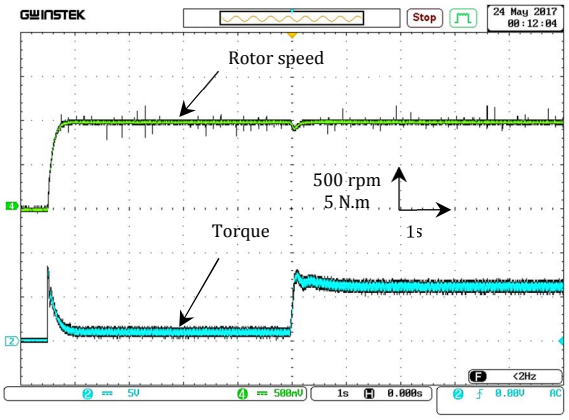


(a) PI-PTC

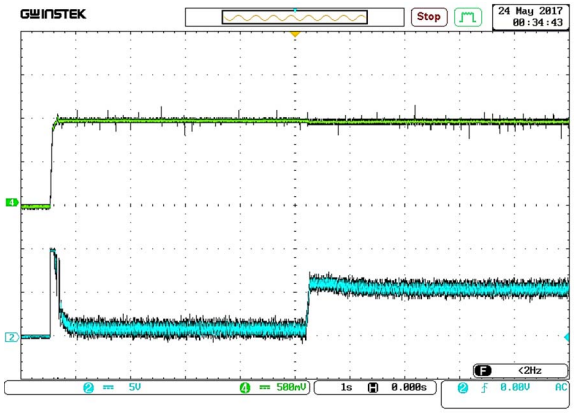

(b) FLC-PTC

Fig.11 Rotor speed and torque at starting up and load application.

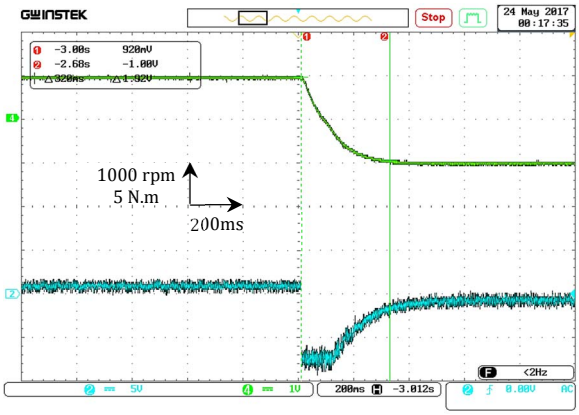


(a) PI-PTC

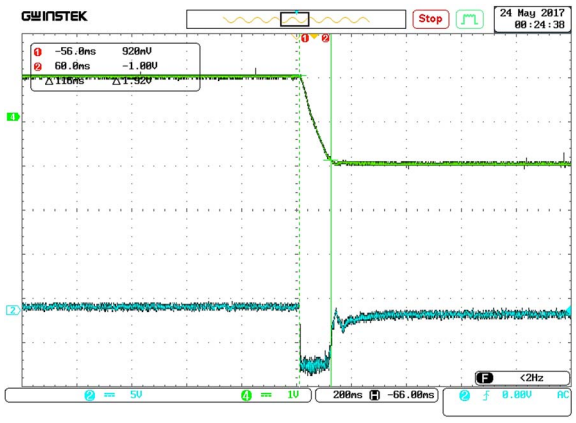


(b) FLC-PTC

Fig.12 Rotor speed and torque during the reversal maneuver.

Fig.11 illustrates the rotor speed and electromagnetic torque in case of two controllers (i.e. PI and FLC) at the starting up stage followed by load application. It is observed that the FLC in Fig.11(b) is much faster in the transient state than PI in Fig.11(a). In addition, it does not show a considerable affection due to load application contrary to the traditional controller which provides an important speed dropping. Furthermore, the torque response of FLC is faster and has less overshoot. Then, in Fig.12 a reversal maneuver has been conducted. This test shows rotor speed and torque responses during the reversing with time calculation which is provided by the numerical oscilloscope. The revising time in case of PI is *320 ms* compared to *116 ms* in case of FLC, this different reflect the high rapidity of fuzzy logic controller in the speed loop than PI.

## VII. Conclusion

In this paper, a comparative evaluation between conventional DTC and finite-state predictive torque control is carried out for two-level voltage inverter fed IM drive. Besides, this paper investigates the use of various speed controllers. All control methods have been verified through real-time implementation using dSpace 1104.

The performances of control have been checked under different operation tests such as steady state, sense reversing and load application. The results indicate that both control strategies have good behavior at steady state and during the reversing. The torque/flux ripples have been considerably reduced in the case of PTC. In addition, the current provides good waveform and less harmonics. Moreover, the results illustrate that the association of PTC scheme with FLC offers more rapidity in transient states and more robustness against external loads which make it a good complementary to PTC strategy to achieve more high performance. Therefore, FS-PTC preserves the good proprieties of DTC especially the simplicity of design. Besides, it can reduce the high ripples. The combination with FLC in speed loop gives more fast and robust response.

## Appendix

The parameters of the Induction motor in SI units are:

*1.1 kW, 50 Hz, p=2, $R_s$=6.75 Ω, $R_r$=6.21 Ω, $L_s$=$L_r$=0.5192 H, $M_{sr}$= 0.4957 H, f=0.002 SI, J=0.01240 kg.m².*

## Reference


[1] I. Takahashi and T. Noguchi, "A New Quick-Response and High-Efficiency Control Strategy of an Induction Motor," *Ind. Appl. IEEE Trans.*, vol. IA-22, no. 5, pp. 820–827, 1986.

[2] D. Casadei, F. Profumo, G. Serra, and A. Tani, "FOC and DTC: Two viable schemes for induction motors torque control," *IEEE Trans. Power Electron.*, vol. 17, no. 5, pp. 779–787, 2002.

[3] V. N. N, A. Panda, and S. P. Singh, "A Three-Level Fuzzy-2 DTC of Induction Motor Drive Using SVPWM," *IEEE Trans. Ind. Electron.*, vol. 63, no. 3, pp. 1467–1479, Mar. 2016.

[4] A. Ammar, A. Benakcha, and A. Bourek, "Closed loop torque SVM-DTC based on robust super twisting speed controller for induction motor drive with efficiency optimization," *Int. J. Hydrogen Energy*, vol. 42, no. 28, pp. 17940–17952, Jul. 2017.

[5] J. Rodriguez, J. Pontt, C. A. Silva, P. Correa, P. Lezana, P. Cortes, and U. Ammann, "Predictive Current Control of a Voltage Source Inverter," *IEEE Trans. Ind. Electron.*, vol. 54, no. 1, pp. 495–503, Feb. 2007.

[6] P. Correa, M. Pacas, and J. Rodriguez, "Predictive Torque Control for Inverter-Fed Induction Machines," *IEEE Trans. Ind. Electron.*, vol. 54, no. 2, pp. 1073–1079, Apr. 2007.

[7] S. Vazquez, J. Rodriguez, M. Rivera, L. G. Franquelo, and M. Norambuena, "Model Predictive Control for Power Converters and Drives: Advances and Trends," *IEEE Trans. Ind. Electron.*, vol. 64, no. 2, pp. 935–947, Feb. 2017.

[8] P. Alkorta, O. Barambones, J. A. Cortajarena, and A. Zubizarrreta, "Efficient Multivariable Generalized Predictive Control for Sensorless Induction Motor Drives," *IEEE Trans. Ind. Electron.*, vol. 61, no. 9, pp. 5126–5134, Sep. 2014.

[9] Y. Zhang, B. Xia, and H. Yang, "Model predictive torque control of induction motor drives with reduced torque ripple," *IET Electr. Power Appl.*, vol. 9, no. 9, pp. 595–604, Nov. 2015.

[10] M. Habibullah and D. D.-C. Lu, "A Speed-Sensorless FS-PTC of Induction Motors Using Extended Kalman Filters," *IEEE Trans. Ind. Electron.*, vol. 62, no. 11, pp. 6765–6778, Nov. 2015.

[11] A. Ammar, A. Bourek, A. Benakcha, and T. Ameid, "Sensorless Stator Field Oriented-Direct Torque Control with SVM for Induction Motor Based on MRAS and Fuzzy Logic Regulation," in *IEEE 6th International Conference on Systems and Control (ICSC)*, 2017, pp. 185–190.

[12] N. R. N. Idris, Chuen Ling Toh, and M. E. Elbuluk, "A New Torque and Flux Controller for Direct Torque Control of Induction Machines," *IEEE Trans. Ind. Appl.*, vol. 42, no. 6, pp. 1358–1366, 2006.

[13] Fengxiang Wang, Zhe Chen, P. Stolze, J. Stumper, J. Rodriguez, and R. Kennel, "Encoderless Finite-State Predictive Torque Control for Induction Machine With a Compensated MRAS," *IEEE Trans. Ind. Informatics*, vol. 10, no. 2, pp. 1097–1106, May 2014.

[14] P. Cortes, S. Kouro, B. La Rocca, R. Vargas, J. Rodriguez, J. I. Leon, S. Vazquez, and L. G. Franquelo, "Guidelines for weighting factors design in Model Predictive Control of power converters and drives," in *2009 IEEE International Conference on Industrial Technology*, 2009, pp. 1–7.

[15] F. Wang, S. Li, X. Mei, W. Xie, J. Rodr??guez, and R. M. Kennel, "Model-based predictive direct control strategies for electrical drives: An experimental evaluation of PTC and PCC methods," *IEEE Trans. Ind. Informatics*, vol. 11, no. 3, pp. 671–681, 2015.